A004

Efficiency Comparison for Continuous Mass-lumped and Discontinuous Galerkin Finite-elements for 3D Wave Propagation

S. Minisini* (Shell Global Solutions International BV), E. Zhebel (Shell Global Solutions International BV), A. Kononov (Source Contracting) & W. A. Mulder (Shell Global Solutions International BV / TU Delft)

SUMMARY

The spreading adoption of computationally intensive techniques such as Reverse Time Migration and Full Waveform Inversion increases the need of efficiently solving the three-dimensional wave equation. Common finite-difference discretization schemes lose their accuracy and efficiency in complex geological settings with discontinuities in the
material properties and topography. Finite-elements on tetrahedral meshes follow the interfaces while maintaining their accuracy and can have smaller meshes if the elements are scaled with the velocity. Here, we consider two higher-order finite-element methods that allow for explicit time stepping: the continuous mass-lumped finite-element method (CMLFE) and
the symmetric interior penalty discontinuous Galerkin method (SIPDG). The price paid for the ability to perform explicit time stepping is an increase in computational cost: CMLFE requires a larger number of discretization nodes to preserve accuracy, whereas SIPDG needs additional
fluxes to impose the continuity of the solution. Therefore, it is not obvious which one is more efficient. We compare the two methods in terms of accuracy, stability and computational cost. Experiments on a three-dimensional problem with a dipping interface show that CMLFE and SIPDG have similar stability conditions, accuracy and efficiency, the last being measured as the computational time required to reach a given accuracy of the result.

Introduction

With the increasing complexity of seismic imaging problems, involving complex geological structures, weathered zones, sharp interfaces and topography, the need for more accurate and efficient solution methods of the wave equation increases. This is especially important for computational intensive algorithms such as Reverse Time Migration and Full Waveform Inversion. Here, we focus on the forward modeling that is a significant part of these algorithms. Because finite-difference methods lose their accuracy in complex settings and in case of topography, finite elements on tetrahedral meshes are more attractive. They offer more flexibility and are more accurate if the mesh follows the geometry of the interfaces and of the topography. The standard finite-element discretization of a scalar wave equation requires matrix inversion, even if the explicit time stepping is used. We focus on two methods that can avoid the inversion of the mass matrix: continuous mass-lumped finite elements (CMLFE) (Mulder, 1996; Chin-Joe-Kong et al., 1999) and the symmetric interior-penalty discontinuous Galerkin (SIPDG) method (Grote and Schötzau, 2009). Combining either spatial discretization with the leapfrog time-integration scheme, which is second-order accurate and conditionally stable, leads to a fully explicit scheme. Zhebel et al. (2011) already discussed the accuracy and performance of the continuous mass-lumped elements of various polynomial degrees in a three-dimensional complex model with topography. Here, we compare continuous and discontinuous finite-element methods in terms of accuracy, storage requirements and performance on a 3-D example with a single, dipping interface.

Method

The scalar wave equation for constant-density acoustics reads

$$\frac{1}{c^2(\mathbf{x})}u_{tt}(\mathbf{x},t) - \Delta u(\mathbf{x},t) = s(\mathbf{x},t), \tag{1}$$

with pressure $u(\mathbf{x},t)$ at position $\mathbf{x} \in \Omega \subset \mathbb{R}^3$ and time $t \in [0,T]$, velocity $c(\mathbf{x})$ varying in space and source term $s(\mathbf{x},t)$. The operator Δ denotes the Laplace operator in three dimensions. The boundary conditions can be homogeneous Dirichlet boundary conditions in case of a free surface, homogeneous Neumann boundary conditions for pure reflection, or absorbing boundary conditions when the domain Ω is truncated for computational purposes.

For a continuous Galerkin formulation with homogeneous boundary conditions, we introduce the weak formulation of (1),

$$\int_\Omega \frac{1}{c^2(\mathbf{x})}u_{tt}\, v\, d\Omega + \int_\Omega \nabla u\, \nabla v\, d\Omega - \int_{\delta\Omega} (\mathbf{n}\cdot\nabla u)\, v\, d\Omega = \int_\Omega s\, v\, d\Omega, \tag{2}$$

for all test functions v in a suitable space, where $\delta\Omega$ consists of the set containing internal boundaries between elements $\delta\Omega_{\text{int}}$ and external boundaries $\delta\Omega_{\text{ext}}$. We consider a partition τ_h of the domain Ω such that $\Omega = \sum_{K\in\tau_h} K$, where K are the elements of the partition – tetrahedra in our case. Let $\mathbf{N}_i$, $i = 1,....,N_h$, denote the nodes of the partition τ_h. We choose the test functions to be the Lagrange polynomials ϕ_j, $j = 1,..,N_h$, with $\phi_j(\mathbf{N}_i) = \delta_{ij}$,$i,j = 1,...,N_h$, where $\delta_{ij} = 1$ if $i = j$ and $\delta_{ij} = 0$ if $i \neq j$. We express the functions v and u in (2) as a linear combination of the Lagrange polynomials: $v(\mathbf{x}) = \sum_{i=1}^{N_h} v_i\, \phi_i(\mathbf{x})$, $u(\mathbf{x},t) = \sum_{j=1}^{N_h} u_j(t)\, \phi_j(\mathbf{x})$. Substituting this representation in (2), we obtain the system of second-order ordinary differential equations

$$\mathbb{M}\mathbf{u}_{tt} + \mathbb{K}\mathbf{u} = \mathbf{s}, \tag{3}$$

where $\mathbb{M}$ denotes the mass matrix with elements $\mathbb{M}_{i,j} = \int_\Omega \phi_i\, \phi_j\, d\Omega$, $\mathbb{K}$ is the stiffness matrix and $\mathbf{s}$ represents the source. For the continuous mass-lumped finite elements, the matrix $\mathbb{M}$ is diagonal. To avoid loss of accuracy compared to the original discretization with the full matrix, polynomials of higher degree in the interior of the faces and of the element have to be included, except for the element of first

degree $M = 1$. In 3D on tetrahedra, we have an element of degree 1, of degree 2 that requires additional polynomials of degree 4 on the faces and in the interior (Mulder, 1996), and two different elements of degree 3 augmented with polynomials of degree 5 on the faces and 6 in the interior (Chin-Joe-Kong et al., 1999). Elements of higher degree are unknown at present. Due to the continuity, the third term in (2) vanishes on the internal boundaries between the elements $\delta\Omega_{\text{int}}$ and the stiffness matrix consists of the second term in (2), $\mathbb{K}_{i,j} = \int_\Omega \nabla\phi_i \, \nabla\phi_j \, d\Omega$. The structure of the stiffness matrix for continuous mass-lumped elements is described elsewhere (Zhebel et al., 2011).

In case of a discontinuous Galerkin discretization, the solution u can be discontinuous at the boundary between neighbouring elements and the third term in (2) does not vanish. We consider the symmetric interior penalty discontinuous Galerkin (SIPDG) discretization (Grote and Schötzau, 2009) with a weak formulation given by

$$\int_\Omega \frac{1}{c^2(\mathbf{x})} u_{tt} \, v \, d\Omega + \int_\Omega \nabla u \, \nabla v \, d\Omega - \int_{\delta\Omega_{\text{int}}} [u]\{\nabla v\} \, d\Omega - \int_{\delta\Omega_{\text{int}}} [v]\{\nabla u\} \, d\Omega + \gamma \int_{\delta\Omega_{\text{int}}} [u][v] \, d\Omega = \int_\Omega s \, v \, d\Omega,$$

where $[u] := u^+ - u^-$ is the jump across the element boundary, $\{u\} := \frac{1}{2}(u^+ + u^-)$ is the average of a function, and γ is a penalty parameter defined as $\gamma = (M+1)(M+2)(M+3)/(6\mathscr{A})$, where M is the degree of the finite element and $\mathscr{A}$ is the area of a face (Minisini et al., 2011). Discretizing the weak formulation, we obtain for each element

$$\mathbb{M}\mathbf{u}_{tt} + \mathbb{K}\mathbf{u} + \mathbb{F}^+\mathbf{u} + \mathbb{F}^-\mathbf{u}^- = \mathbf{s}, \tag{4}$$

where $\mathbb{M}$ and $\mathbb{K}$ are the local mass and stiffness matrix, respectively, both of dimension $N_{DG} \times N_{DG}$, with $N_{DG} = (M+1)(M+2)(M+3)/6$; $\mathbf{u}^-$ denotes the solution on one of the neighbouring elements. We also have the contribution of the fluxes. The term $\mathbb{F}^+$ denotes the sum of outgoing fluxes over faces in the given element. The second term $\mathbb{F}^-$ contains incoming fluxes from the four neighbouring elements.

The discretization in space with the continuous mass-lumped elements or the SIPDG method leads to a linear system of second-order ordinary differential equations, (3) or (4). By choosing a symmetric time-marching scheme, for example leapfrog, we obtain a fully algebraic system for the continuous mass-lumped elements,

$$\mathbf{u}_{n+1} = 2\mathbf{u}_n - \mathbf{u}_{n-1} + \Delta t^2 \, \mathbb{M}^{-1} \left(-\mathbb{K}\mathbf{u}_n + \mathbf{s}_n\right), \tag{5}$$

for SIPDG, for each element, we obtain

$$\mathbf{u}_{n+1} = 2\mathbf{u}_n - \mathbf{u}_{n-1} + \Delta t^2 \, \mathbb{M}^{-1} \left(-\mathbb{K}\mathbf{u}_n - \mathbb{F}^+\mathbf{u}_n - \mathbb{F}^-\mathbf{u}_n^- + \mathbf{s}_n\right). \tag{6}$$

The only unknown is the vector $\mathbf{u}_{n+1}$. The values of the solution at the previous time steps n and $n-1$ are known. In the case of mass-lumped elements, the global mass matrix is diagonal and trivial to invert. In the case of SIPDG, the global mass matrix is block diagonal and also easily inverted. Higher-order time-stepping methods can be readily implemented (Dablain, 1986).

Results

We will compare the continuous mass-lumped and SIPDG finite element methods in terms of accuracy, stability and computational cost. The stability constraint for time stepping requires an estimate of the spectral radius of the spatial operator, which in the continuous case consists of the stiffness matrix left-multiplied by the inverse of the diagonal mass matrix. In the SIPDG case, the spatial operator also includes the fluxes and the global mass matrix is block-diagonal. The stability condition for time stepping can be expressed as $\Delta t \leq \texttt{CFL}\,(d/c)_{\min}$ where $(d/c)_{\min}$ is the minimum over all elements of the ratio of the diameter d of the inscribed sphere and the velocity c per element. The Courant-Friedrichs-Lewy number can be taken as $\texttt{CFL} = 2/(d\sqrt{\rho_s})$, using the spectral radius ρ_s of the spatial operator and the largest diameter d of the inscribed spheres of the elements, evaluated for a simpler constant-velocity case. For these simpler case, we have considered (i) the single reference element with Neumann

Table 1 *CFL condition for different degrees computed on the reference tetrahedron.*

	CFL	
degree *M*	mass-lumped	SIPDG
1	1.18	0.168
2	0.090	0.091
3 (1)	0.059	0.0596
3 (2)	0.102	
4		0.0404

Table 2 *Comparison of the number of nodes for mass-lumped and SIPDG elements.*

degree *M*	mass-lumped			DG
	compute	store	global	
1	4	0.17	4.0	4
2	23	8.5	6.7	10
3	50	25	9.2	20
4				35

boundary conditions, (ii) the unit cube that can be partitioned into 6 tetrahedra and (iii) its periodic extension using Fourier stability analysis. This provides necessary, but perhaps not sufficient, stability conditions. Table 1 lists the worst-case results of these three cases for continuous mass-lumped and SIPDG elements. The first-degree mass-lumped elements have a much larger CFL, resulting in a larger allowable time step and in less computational time than required for SIPDG. The CFL for elements of second degree are comparable for both schemes. The second type of the third-degree mass-lumped element is more efficient than the first type and allows for a larger time step then required with SIPDG. Since mass-lumped elements of degree 4 and higher are presently unknown, only the stability result for SIPDG is given. The general trend for SIPDG is that CFL becomes smaller for higher-order elements.

To compare accuracy and performance, we need a problem that has an exact solution. We consider a three-dimensional domain of size $(2\text{ km})^3$ with two halfspaces having velocities of 1.5 and 3.0 km/s. The interface runs from 0.7 to 1.3 km depth between 0 and 2 km in x, so the dip angle is 16.7°. A shot is located at (779.7, 1000, 516.3) m, 350 m above the interface in the shallow low-velocity part of the model. The receivers are located 250 m above the interface and have offsets from 100 to 700 m with a 25-m interval, parallel to the interface in the down-dip direction of the source, see Figure 1. We subtracted the direct wave by replacing the velocity model with a constant velocity of 1.5 km/s and subtracting the computed traces from those obtained for original model. The timestep was kept the same, as was the mesh. In this way, the numerical errors in the direct wave are removed as well. The resulting reflected wave was then compared to the exact solution. The Figure 3 shows the accuracy and the computational performance, the last being measured as the computational time required to reach a given accuracy of the result.

Table 2 lists the number of nodes per element. In the DG case, due to the local formulation for each element, the number of nodes per element listed in the last column, is the same for computation and storage. The continuous elements have a larger number of nodes per element, listed in column 2. Since nodes on vertices, edges and faces are shared, the effective number of nodes that needs to be stored per

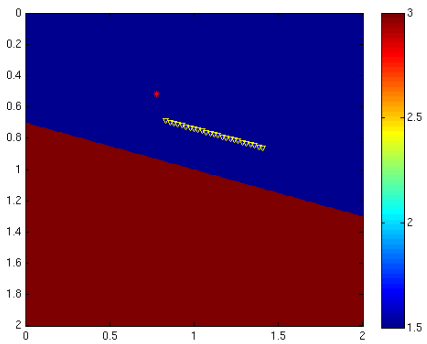

Figure 1 *Velocity model. The source is denoted by a red star and receivers by yellow triangles.*

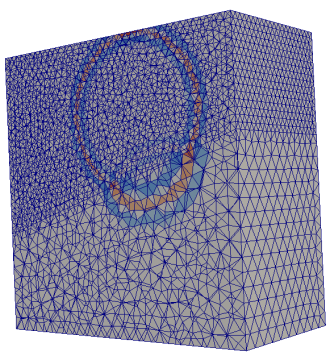

Figure 2 *Snapshot of the wave field.*

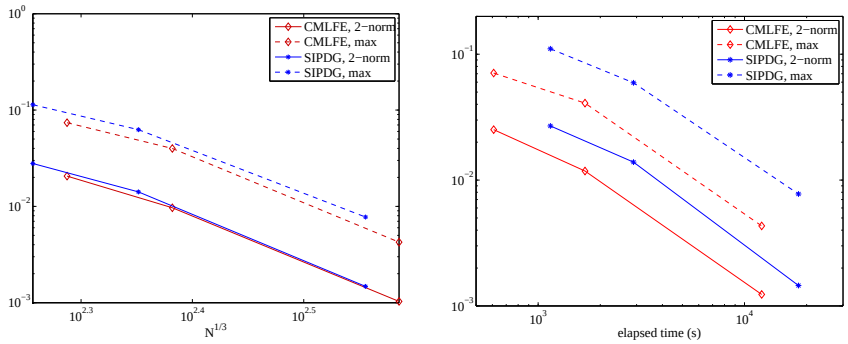

(a) (b)

Figure 3 *(a) Absolute error as a function of $N^{1/3}$, where is N is the number of degrees of freedom for CMLFE or SIPDG of degree 3. The dashed lines represent the maximum norm, the drawn the 2-norm. (b) Absolute error as a function of computational time on 12 cores using OpenMP. To save storage the mass and stiffness matrices are recomputed each time step.*

element is smaller, as can be seen in the third column, obtained by taking the observed number of degrees of freedom divided by the number of elements for the finest mesh used in this comparison. If the stiffness matrix is computed on the fly at each time step to save storage, the cost of assembly per element will depend on number of nodes per element, as given in column 2 for the continuous case and column 5 for DG. If the global stiffness matrix is assembled in the continuous case, the effective number of nodes to store is listed in the fourth column, being the square root of the average number of columns per degree of freedom. The results show that in case of global assembly of the stiffness matrix, the continuous mass-lumped finite elements require less storage than SIPDG. When the stiffness matrix is computed on the fly during each time step, the two methods require a similar amount of storage, determined mainly by the unknowns that describe the wavefield at two consecutive time steps, the velocity model and the data structure that describes the tetrahedra.

Conclusions

We have compared the continuous mass-lumped finite-element method (CMLFE) to the symmetric interior penalty discontinuous Galerkin method (SIPDG) in terms of accuracy, stability and computational performance. Both methods are combined with a time-marching scheme that leads to a fully explicit formulation. The stability analysis for time stepping has shown that both methods have comparable stability limits, except for elements of degree 1 and second type of degree 3, where CMLFE has more favourable time-stepping stability limit. Experiments on a 3-D problem with dipping interface show that CMLFE and SIPDG have similar accuracy, but CMLFE is faster due to its larger allowable time step.

References

Chin-Joe-Kong, M.J.S., Mulder, W.A. and van Veldhuizen, M. [1999] Higher-order triangular and tetrahedral finite elements with mass lumping for solving the wave equation. *Journal of Engineering Mathematics*, **35**(4), 405–426, doi:10.1023/A:1004420829610.

Dablain, M.A. [1986] The application of high-order differencing to the scalar wave equation. *Geophysics*, **51**(1), 54–66, doi:10.1190/1.1442040.

Grote, M.J. and Schötzau, D. [2009] Optimal error estimates for the fully discrete interior penalty DG method for the wave equation. *Journal of Scientific Computing*, **40**(1–3), 257–272, doi:10.1007/s10915-008-9247-z.

Minisini, S., Zhebel, E., Kononov, A. and Mulder, W.A. [2011] A comparison of 3-D explicit continuous and discontinuous Galerkin methods for the second-order wave equation. *Numerical Linear Algebra and Applications*, submitted.

Mulder, W.A. [1996] A comparison between higher-order finite elements and finite differences for solving the wave equation. *Proceedings of the Second ECCOMAS Conference on Numerical Methods in Engineering*, John Wiley & Sons, Chichester, 344–350.

Zhebel, E., Minisini, S., Kononov, A. and Mulder, W.A. [2011] Solving the 3D acoustic wave equation with higher-order mass-lumped tetrahedral finite elements. 73rd EAGE Conference & Exhibition, Extended Abstracts, A010, Vienna, Austria.